

# Mathematical Models of Human Sinus and Atrioventricular Node Action Potentials

S Inada, MR Boyett, H Dobrzynski

University of Manchester, UK

## Abstract

There are few models of the human cardiac action potential, because it is difficult to obtain human heart for electrophysiological study. In this study, we have developed action potential models for human sinus node and atrioventricular junction based on the expression of ion channel messenger RNAs (mRNAs). The computed action potentials for the seven regions had feasible characteristics and shapes. Although function is not necessarily linearly related to mRNA abundance, we suggest this technique is a new form of bioinformatics to explore the consequences of a change in ion channel expression, e.g. in aged or diseased heart.

## 1. Introduction

Because of few electrophysiological studies of human heart, it is difficult to construct mathematical models of

human heart action potentials. Recently, we have measured the expression of ion channel messenger RNAs (mRNAs) in human sinus and atrioventricular nodes using quantitative polymerase chain reaction (qPCR) [1]. The purpose of this study was to construct action potential models for the sinus node, paranodal area, and atrioventricular junction (transitional zone, inferior nodal extension, atrioventricular node, penetrating bundle and ventricle) from these data.

## 2. Methods

A model of the human action potential was developed based on the model of Courtemanche et al. of the right atrial action potential (based on extensive electrophysiological data from human right atrium) [2]. It was assumed that whole cell conductance for a particular ionic current is roughly proportional to the abundance of one or more mRNAs responsible for the relevant ion channel, ignoring the possible non-linearity of the

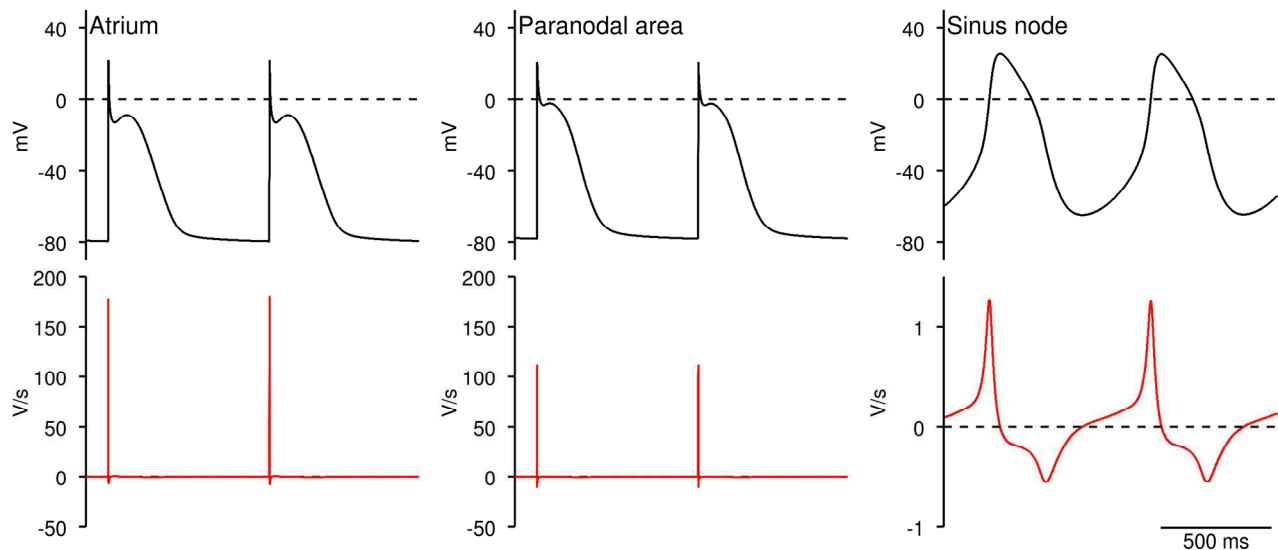


Figure 1. Action potentials of the sinus node and paranodal area. Atrial action potential as calculated according to the model of Courtemanche et al. (left) and paranodal area and sinus node action potentials as calculated with the modified model of Courtemanche et al. (middle and right). Membrane potential is shown in top panels, rate of change of membrane potential ( $dV/dt$ ) in bottom panels.

relationship between mRNA abundance and conductance. For each of the major ionic currents ( $I_{Na}$ ,  $I_{Ca,L}$ ,  $I_{to}$ ,  $I_{Kur}$ ,  $I_{Kr}$ ,  $I_{Ks}$  and  $I_{K1}$ ), the sum of relevant mRNAs in the sinus node, paranodal area, and the atrioventricular junction were calculated and expressed as a percentage of the sum of the same mRNAs in the right atrium. This was assumed to be equal to the conductance of the relevant ionic current in the sinus node, paranodal area and the atrioventricular junction expressed as a percent of the conductance in the right atrium. The Courtemanche model does not include T-type calcium current ( $I_{Ca,T}$ ) and hyperpolarized-activated current ( $I_f$ ) and yet the nodal tissues express the relevant ion channels. Therefore, conductance for  $I_{Ca,T}$  was assumed to be the same as in rabbit sinus node cell model by Zhang et al. [3], and conductance for  $I_f$  was taken from the study of human sinus node by Verkerk et al [4]. Whereas in atria,  $Ca_v1.2$  mRNA is the principal L-type  $Ca^{2+}$  channel isoform mRNA, in the sinus node,  $Ca_v1.3$  mRNA accounts for 16% of the total. In the sinus node, it was assumed that the activation curve of  $Ca_v1.3$ -dependent  $I_{Ca,L}$  is shifted by -20 mV compared to the activation curve of  $Ca_v1.2$ -dependent  $I_{Ca,L}$ . The data from  $K_{ir2.1}$ ,  $K_{ir2.2}$  and  $K_{ir2.3}$  ( $K^+$  channels responsible for  $I_{K1}$ ) were scaled to account for the different single channel conductances of the three channels. As well as the ionic currents, three  $Ca^{2+}$ -handling process in the Courtemanche et al. model were modified:  $Na^+$ - $Ca^{2+}$  exchange, sarcoplasmic reticulum (SR)  $Ca^{2+}$  release and SR  $Ca^{2+}$  uptake. They were modified in an analogous manner: mRNA for NCX1 (responsible for  $Na^+$ - $Ca^{2+}$  exchange), RyR2 (responsible

for SR  $Ca^{2+}$  release) and SERCA2a (responsible for SR  $Ca^{2+}$  uptake) in the sinus node was expressed as a percentage of same mRNAs in the right atrium. Whereas a right atrial cell was assumed to have a capacitance of 100 pF and a volume of 20,100  $\mu m^3$ , a cell of sinus node, inferior nodal extension and atrioventricular node were assumed to have a capacitance of 50 pF and volume of 10,050  $\mu m^3$ . Models for the action potential in the other areas were constructed in the same manner, a cell in the paranodal area, transitional area and penetrating bundle were assumed to have a capacitance of 75 pF and a volume of 15,075  $\mu m^3$ , a cell in the ventricle was assumed to have the same capacitance and volume as the atrial cell.

To estimate the conduction velocity in the atrioventricular junction, we simulated action potential conduction using the one-dimensional string of cells (Figure 3A top). The one-dimensional string was composed of cell in atrium, transitional area, inferior nodal extension, atrioventricular node, penetrating bundle or ventricle. Neighbouring cells in the one-dimensional string were electrically coupled by a coupling conductance. In the one-dimensional string of atrial cells, the coupling conductance was set to 1,000 nS (giving a conduction velocity of 52.7 cm/s). In the case of the one-dimensional strings of other cell types, the coupling conductance was scaled depending on the abundance of mRNAs for Cx40, Cx43 and Cx45. The mRNA abundance of Cx40, Cx43 and Cx45 were scaled (multiplied) to account for the different single channel

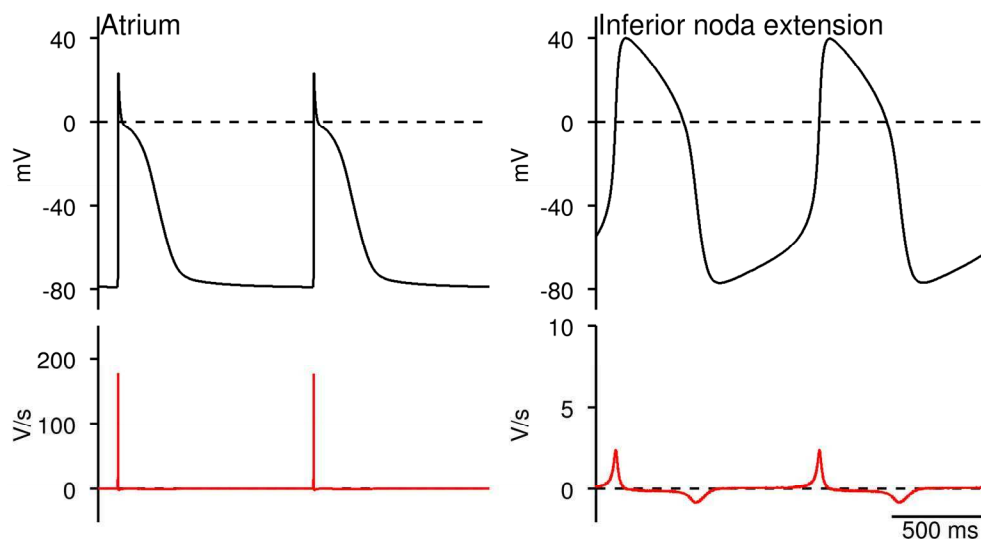


Figure 2. Action potentials at the atrioventricular junction. Atrial action potential as calculated according to the model of Courtemanche et al (left), inferior nodal extension (right) with the modified model of Courtemanche et al. Membrane potential is shown in top panels, rate of change of membrane potential (dV/dt) in bottom panels. Note that in this simulations, conductance for  $I_{to}$  decreased up to 30% in all tissue.

conductance of the three channels (Cx40 – 200 pS; Cx43 – 80 pS; Cx45 – 30 pS [5]) before they were summed. The end of a string was stimulated and the conduction time along the string was measured.

### 3. Results

The calculated atrial action potential from the unmodified model of Courtemanche et al. and the calculated sinus node and paranodal area action potentials as predicted from the model are shown in Figure 1. The trace produced in the sinus node is a typical pacemaker action potential with a slow upstroke velocity. The action potential in the paranodal area was modeled in the same way as the sinus node action potential; compared with the atrial action potential, the upstroke velocity and amplitude of the action potential were reduced, and the membrane tended to be depolarized during diastole.

Figure 2 shows the computed action potential and rate of change of membrane potential for the atrial cell, calculated using the model of Courtemanche et al., as well as the inferior nodal extension calculated using the modified model. Note that in this simulation, conductance for  $I_{to}$  decreased up to 30% in both tissue. The transitional area is predicted to have a transitional action potential, the inferior nodal extension and atrioventricular node typical nodal action potential, and the penetrating bundle fast upstroke action potential. The predicted ventricular action potential has the roughly expected form. The maximum upstroke velocity of the action potential ( $dV/dt_{max}$ ), which is high in the atrium (124 V/s), is predicted to be lower in the transitional area (35 V/s), low in the inferior nodal extension and atrioventricular node (2-12 V/s), and high in the penetrating bundle and ventricle (>130 V/s).  $dV/dt_{max}$  is known to be low along the atrioventricular conduction axis. During diastole, in the atrium, there is a stable

resting potential. It is predicted that in the ventricle there is also a stable resting potential, where in the transitional area and penetrating bundle the membrane is more depolarized and less stable. In contrast, in the inferior nodal extension and atrioventricular node, it is predicted that there is a slow depolarization during diastole. It is predicted that the inferior nodal extension and atrioventricular node are both capable of pacemaker activity with cycle length of 1042 and 877 ms, respectively. This is consistent with the finding that, in the human heart, the leading pacemaker site at the atrioventricular junction is in the atrioventricular node and its junction with the penetrating bundle.

We calculated the conduction time of the action potential along a string of 300 electrically coupled cells (Figure 3A top). In the case of atrial myocytes, the coupling conductance (1000 nS) was chosen to give an appropriate conduction velocity (53 cm/s). The coupling conductance was scaled based on the expression of connexion mRNAs for each region. The predicted conduction velocity was low in the inferior nodal extension (Figure 3B). In the inferior nodal extension, the predicted conduction velocity was 9 cm/s, similar to that recorded experimentally in the rabbit.

### 4. Discussion and conclusions

The computed action potentials for the seven regions had feasible characteristics and shapes. It is predicted that human ventricle has a fast upstroke and a stable resting potential and does not show pacemaker activity. In contrast, it is predicted that human sinus and atrioventricular nodes have a slowly conducting action potential with a slow upstroke and diastolic depolarization and do show pacemaker activity.

A major factor determining the conduction velocity of the action potential is the coupling conductance, which is

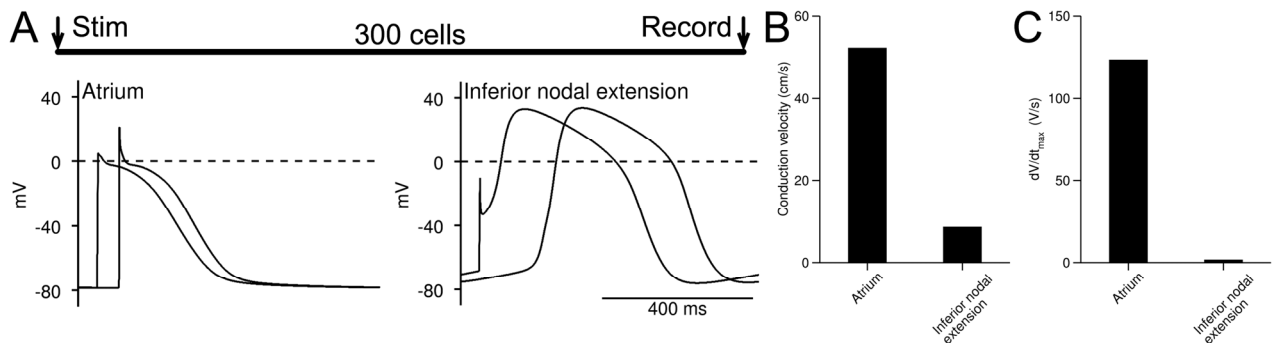


Figure 3. Predicted action potential conduction based on qPCR data (Chandler et al.). A, calculation conduction velocity. One end of string of 300 electrically-coupled cells was stimulated. Pairs action potential (recorded at stimulation site and distal end of string) shown. B, conduction velocity calculated from interval between two action potentials (assuming cells are 100  $\mu$ m in length and joined end to end). C, calculated upstroke velocity of action potential ( $dV/dt_{max}$ ).

determined by the expression of connexins. Cx43 mRNA and protein, responsible for medium conductance channels, were poorly expressed in the atrioventricular node, inferior nodal extension and penetrating bundle as compared to the working myocardium. Cx40 mRNA, responsible for large conductance channels, also tended to be more poorly expressed in the atrioventricular node and inferior nodal extension. Another major factor determining the conduction velocity is the upstroke velocity of the action potential (Figure 3C), which is determined by the expression of the cardiac Na<sup>+</sup> channel. Together the expression of connexins and Na<sup>+</sup> channel can explain the variation in the conduction velocity along the atrioventricular axis: the conduction velocity is predicted to be slowest in the inferior nodal extension and highest in the penetrating bundle.

In this study, we have developed action potential models of the human heart in various regions from atrial action potential model and mRNAs expression. Although function is not necessarily linearly related to mRNA abundance, we suggest this technique is a new form of bioinformatics to explore the consequences of a change in ion channel expression, e.g. in aged and diseased heart.

## References

- [1] Chandler NJ, Greener ID, Tellez JO, Inada S, Musa H, Molenaar, P, DiFrancesco, D, Bruscott, M, Longhi R, Anderson RH, Billeter R, Sharma V, Sigg DC, Boyett MR, Dobrzynski H. Molecular Architecture of the Human Sinus node. Insights Into the Function of the Cardiac Pacemaker. *Circulation*. 2009;119:1562-1575.
- [2] Courtemanche M, Ramirez RJ, Nattel S. Ionic Mechanisms Underlying Human Atrial Action Potential Properties: Insights from a Mathematical Model. *Am J Physiol*. 1998;275:H301-H321.
- [3] Zhang H, Holden AV, Kodama I, Honjo H, Lei M, Verghese T, Boyett MR. Mathematical Models of Action Potentials in the Periphery and Center of the Rabbit Sinoatrial Node. *Am J Physiol*. 2000;H397-H421.
- [4] Verkerk AO, van Borren MM, Peters RJ, Broekhuis E, Lam KY, Coronel R, de Bekker JM, Tan HL, Wilders R. Single cells isolated from human sinoatrial node. *Conf Proc IEEE Eng Med Biol Soc*. 2007;1:904-907.
- [5] Boyett MR, Inada S, Yoo S, Li J, Liu J, Tellez JO, Greener ID, Honjo H, Billeter R, Lei M, Zhang H, Efimov IR, Dobrzynski H. Connexins in the sinoatrial node and atrioventricular nodes. *Advances in Cardiology*. 2006;42:175-197.

Address for correspondence

Dr. Halina Dobrzynski  
Cardiovascular Research Group, Core Technology Facility, 46  
Grafton Street, University of Manchester, M13 9NT, UK  
halina.dobrzynski@manchester.ac.uk